## ARTICLES

# High-precision calculation of the equation of state and crystallographic phase stability for aluminum

J. C. Boettger
*Theoretical Division, Los Alamos National Laboratory, Los Alamos, New Mexico 87545*

S. B. Trickey
*Quantum Theory Project, Departments of Physics and of Chemistry, University of Florida, Gainesville, Florida 32611*
(Received 24 July 1995; revised manuscript received 20 September 1995)

High-precision, all-electron, full-potential, local-density approximation (LDA) calculations are used to determine the static lattice equation of state (EOS) and crystalline phase stability of Al to 1 TPa. The low-pressure properties found here are consistent with the results of other nonrelativistic LDA calculations, but differ significantly from the results of relativistic LDA or gradient-dependent approximation calculations. The theoretical 300-K isotherm for fcc Al, obtained by adding phonon effects to the static lattice EOS, is in reasonable agreement with room temperature data up to 220 GPa. The predicted static-lattice phase sequence for Al is fcc→hcp→bcc with the transitions occurring at 205±20 GPa and 565±60 GPa. Estimation of the possible impact of phonons on the fcc→hcp transition produces a fairly firm upper bound of 290 GPa (282) on the room-temperature (zero temperature) fcc→hcp transition pressure. This result suggests that a recent diamond-anvil-cell experiment came very close to achieving the fcc→hcp transition.

## I. INTRODUCTION

The equation of state (EOS) and structural phase stability of Al were the subject of three theoretical investigations[1–3] more than a decade ago which used the local-density approximation (LDA) to density-functional theory. In the first of those studies, McMahan and Moriarity[1] calculated the relative stabilities of the fcc, hcp, and bcc crystal structures using two distinct methods to solve the Kohn-Sham equations: the generalized pseudopotential technique (GPT) and the all-electron linear muffin-tin-orbital (LMTO) method within the so-called atomic-sphere approximation (ASA). Although the two methods produced the same phase sequence, fcc→hcp→bcc, the predicted transition pressures were notably different; 360 and 560 GPa, respectively, from GPT versus 120 and 200 GPa from LMTO-ASA. In the second investigation, Lam and Cohen[2] repeated the earlier calculations using the *ab initio* pseudopotential (AP) method. They found the same sequence of structures with yet another set of predicted transition pressures; 220 and 380 GPa.[4] Since the extreme values for the transition pressures were obtained in a single study using the same LDA, Hedin-Lundqvist,[5] it was clear that the wide variation in the results had to be attributed to algorithmic differences among the calculations.

To address the discrepancies among the various predictions, the structural phase stability of Al was examined a third time using the all-electron, full-potential linear combination of Gaussian-type orbitals (LCGTO) method,[3] together with the simple Kohn-Sham-Gaspar LDA.[6] Although the LCGTO method employs fewer approximations than the techniques used in the earlier calculations, the particular LCGTO code used then was restricted to cubically symmetric lattices. The third investigation was only able to address the hypothetical fcc→bcc transition therefore. The predicted transition pressure, 330 GPa,[3] agreed well with the AP value of 300 GPa.[2] On the basis of that agreement, it was concluded[3] that the best available predictions for the physically realizable transitions in Al were those produced with the AP method.

At the time of the three theoretical studies discussed no experimental data were available in the pressure range of interest. That condition has since changed. A new measurement of the room-temperature equation of state (EOS) and crystal structure of Al using diamond-anvil-cell (DAC) techniques[7] found that the fcc structure remains stable up to 219 GPa ($V/V_0=0.50$). Thus, neglecting metastability, $P_{\mathrm{fcc}\rightarrow\mathrm{hcp}}\geqslant 220$ GPa. This measurement had serious implications for interpretation of the prior calculations.[8] If the lowest predicted fcc→hcp transition pressure (120 GPa, LMTO)[1] were to be the actual LDA value, there would be a serious conflict between experiment and theory. If on the other hand, the highest predicted pressure (360 GPa, GPT)[1] were to be the correct LDA value, the predicted transition would lie at such an elevated pressure that there would be little hope of observing it in the near future. If the intermediate prediction (220 GPa, AP)[2] were to be correct, the DAC experiment came extremely close to achieving the fcc→hcp transition, and should be pursued vigorously.

This phase transition pressure was the focus of a recent paper.[8] There we showed that high-precision, all-electron, full-potential calculations using the linear combination of Gaussian-type orbitals-fitting function (LCGTO-FF) technique, combined with a rough estimate for the impact of zero-point motion on the transition, place a fairly firm

 

upper bound of 290 GPa on the $T=0$ K fcc→hcp phase transition in Al. Those results suggested that there is no inherent conflict between the accurate LDA prediction and the experimental result, *so long as thermal effects on the room-temperature phase transition are negligible*.

Here, we go substantially beyond the preliminary report to include a number of new results and insights based on the entire calculated EOS's for all three phases of Al. Simple analytical EOS's that are accurate fits to the calculated static lattice EOS's of fcc, hcp, and bcc Al for pressures ranging up to 450 GPa are presented. A detailed comparison of the calculated low-pressure properties of fcc Al with experimental data and with theoretical results obtained using a wide range of computational techniques and density-functional models provides new insights into systematic differences between the various types of models. In addition, our LCGTO-FF results for the zero-pressure properties of hcp and bcc Al are presented. A theoretical 300-K isotherm for fcc Al is calculated by incorporating thermal nuclear effects into the static lattice 0-K isotherm and is compared with room-temperature data up to 220 GPa. Finally, an upper bound is placed on the *room-temperature fcc→hcp* phase transition pressure by estimating the possible impact of phonons on that transition.

## II. COMPUTATIONAL DETAILS

The present calculations employed the LCGTO-FF technique, as embodied in the computer program GTOFF,[9] a generalization [to include one-dimensional (1D) and 3D periodicity] of the 2D electronic structure program FILMS.[10,11] The LCGTO-FF method is an all-electron, full-potential technique for solving the one-electron equations that is characterized by its use of three independent GTO basis sets to expand the orbitals, charge density, and LDA exchange-correlation (XC) kernels. (The LDA parametrization of Hedin and Lundqvist is used here;[5] see below.) The charge fitting functions are used to reduce the total number of Coulomb integrals by replacing the usual four-center integrals in the total energy and one-electron equations with three-center integrals. The XC fit provides a simple yet sophisticated numerical quadrature scheme capable of producing accurate results with a rather coarse numerical integration mesh.

The orbital, charge, and XC basis sets used here were derived from the ''interior layer'' basis sets developed and tested during recent studies of Al ultrathin films[12] and Na adsorption on the Al(111) surface.[13] The only modifications made in those basis sets were (1) The $p$- and $d$-type fitting functions were eliminated since they lack the correct rotational symmetry for the cubic systems, and (2) For the three smallest volumes considered here, the smallest exponents were increased to avoid approximate linear dependencies. For any given molar volume, the basis sets used for the fcc, hcp, and bcc structures were required to be identical.

The Brillouin-zone (BZ) integrations employed uniform meshes which preserve the lattice symmetry with 72 and 76 points in the irreducible wedges of the cubic and hcp BZ's, respectively. The BZ integrations were performed via a broadened histogram technique, with the DOS for each calculated state approximated by a normalized Gaussian with a width of 20 mRy. The accuracy of the histogram integrations was tested in a series of calculations using the linear tetrahedral method with the integrations performed over the full BZ to ensure that the correct star weights for the irreducible **k** points were generated.[14] Fully converged results were then estimated by the extrapolation technique of Jansen and Freeman[15] using BZ meshes with up to about 400 points in the irreducible wedge. Those authors had found Al to be a particularly slowly converging system with respect to BZ scan density. Our tests confirm that behavior, a finding which suggests that the linear tetrahedral integration used in the previous LCGTO work on bulk Al,[3] with less than 150 irreducible **k** points for each structure, was not as precise as the current BZ integrations.

## III. RESULTS

Total energies were calculated for fcc, hcp, and bcc Al at 12, 10, and 10 lattice constants, respectively. The hcp phase was treated at ideal $c/a$ only. Cohesive energies were then determined relative to a spin-polarized atomic energy of $-482.596\,646$ Ry, obtained from an expanded lattice calculation using GTOFF. The lattice constants used here and the calculated cohesive energies are given in Table I. The zero-pressure properties, EOS, and crystallographic phase stability of Al were then derived from the data in Table I.

### A. Zero-pressure properties

The zero-pressure properties and EOS's up to about 450 GPa for the three phases of Al were obtained by fitting the calculated cohesive energies of the eight largest bcc and hcp volumes and the ten largest fcc volumes with a modified version of the so-called ''universal'' EOS.[16] The modification consists of removing the constraint that the fitted cohesive energy must vanish for arbitrarily large lattice constants, which is irrelevant in the present context. The functional form used here was

$$E_c(a) = -(E_0+E_1) + E_1\left[1+\frac{(a-a_0)}{l}\right]\exp\left[-\frac{(a-a_0)}{l}\right], \tag{1}$$

where $a_0$ is the zero-pressure lattice constant (in bohr), $E_0$ is the binding energy (negative of cohesive energy, in Ry/atom), and $l$ is a scale length (in bohr). The fourth parameter $E_1$ (in Ry/atom) can be written in terms of the bulk modulus ($B_0$, in GPa);

$$E_1 \equiv -9Cfa_0l^2B_0, \tag{2}$$

where $C=6.797\,865\times10^{-5}$ GPa bohr$^3$/Ry is a unit conversion factor and $f=V_0/a_0^3$ is a structure-dependent constant. The values found here for the four independent parameters ($a_0$, $E_0$, $B_0$, and $l$) are given in Table II for each structure. The rms deviations ($\sigma$) for the three fits are also given in Table II. The relatively small deviations for these fits over a large range of cohesive energies demonstrates the numerical stability achieved with GTOFF and ensures that these analytical EOS's will provide an accurate representation of the calculated static-lattice 0-K isotherms of fcc, hcp, and bcc Al for pressures ranging up to 450 GPa.

Table III compares the zero-pressure static-lattice properties obtained here for the fcc structure of Al with results from

TABLE I. Lattice constants ($a$, bohr) and calculated cohesive energies ($E_c$, Ry/atom) for the fcc, hcp, and bcc structures of Al. Lattice constants for the three phases that lie on the same line correspond to nearly equal molar volumes. The hcp phase is at ideal $c/a$.

| Fcc | | Hcp | | Bcc | |
|---|---|---|---|---|---|
| $a$ | $E_c$ | $a$ | $E_c$ | $a$ | $E_c$ |
| 7.80 | −0.297 576 | 5.515 | −0.294 166 | 6.191 | −0.290 246 |
| 7.70 | −0.298 974 | 5.445 | −0.295 374 | 6.111 | −0.291 036 |
| 7.65 | −0.299 358 | | | | |
| 7.60 | −0.299 460 | 5.374 | −0.295 796 | 6.032 | −0.291 044 |
| 7.55 | −0.299 358 | | | | |
| 7.50 | −0.298 988 | 5.303 | −0.295 299 | 5.953 | −0.290 154 |
| 7.40 | −0.297 422 | 5.233 | −0.293 772 | 5.873 | −0.288 162 |
| 7.00 | −0.277 392 | 4.950 | −0.273 783 | 5.556 | −0.266 956 |
| 6.40 | −0.180 292 | 4.525 | −0.178 108 | 5.080 | −0.171 866 |
| 5.60 | 0.201 730 | 3.960 | 0.194 344 | 4.445 | 0.196 302 |
| 5.35 | 0.428 480 | 3.783 | 0.416 120 | 4.2463 | 0.413 614 |
| 5.105 | 0.730 400 | 3.609 | 0.713 934 | 4.0515 | 0.701 874 |

a wide variety of calculations[3,17–24] using diverse approximations. The theoretical results have been divided into three groups; (1) nonrelativistic LDA calculations, (2) relativistic LDA calculations, and (3) calculations using some form of gradient-dependent approximation (GDA) to density-functional theory. Table III also gives experimental $T=0$ K results for $a_0$ and $E_0$, as deduced from room-temperature data by Refs. 18 and 3, respectively, and an experimental value of $B_0$ from Ref. 7.

Inspection of Table III reveals a number of interesting trends. First, the nonrelativistic LDA calculations, using LDA models that go beyond the simplest KSG approximation, give very good bond lengths and bulk modulii, in spite of having the usual LDA overbinding. (Here, the nonrelativistic LDA result from Ref. 19 is discarded as being clearly anomalous.) When the KSG model is used, the binding energy is reduced to roughly the experimental value, while the lattice constant becomes slightly expanded. Given the fact that the first three nonrelativistic LDA entries in Table III include a pseudopotential calculation,[18] an all-electron, muffin-tin potential calculation,[17] and the current all-electron, full-potential results, there is a remarkable degree of consistency in the results. Taking into consideration the varying degrees of approximation used in those three calcu-

TABLE II. Modified universal EOS parameters for the fcc, hcp, and bcc phases of Al; equilibrium lattice constant ($a_0$, bohr), binding energy ($E_0$, Ry/atom), bulk modulus ($B_0$, GPa), and scale length ($l$, bohr), along with the standard deviation ($\sigma$, Ry/atom) for each fit.

| | Fcc | Hcp | Bcc |
|---|---|---|---|
| $a_0$ | 7.596 49 | 5.376 55 | 6.077 27 |
| $E_0$ | 0.299 420 | 0.295 782 | 0.291 119 |
| $B_0$ | 79.658 4 | 77.652 8 | 68.769 9 |
| $l$ | 1.405 24 | 1.001 34 | 1.094 65 |
| $\sigma$ | 0.000 047 | 0.000 032 | 0.000 083 |

TABLE III. The lattice constant ($a_0$, bohr), static lattice binding energy ($E_0$, eV/atom), and bulk modulus ($B_0$, GPa) for the fcc structure of Al. Calculated results are separated into three groups; nonrelativistic LDA, relativistic LDA, and GDA. The type of DFT approximation used for each calculation is also indicated; HL=Hedin-Lundqvist, W=Wigner correlation, KSG=Kohn-Sham-Gaspar, PZ=Perdew-Zunger, PW91 (PW86)=Perdew-Wang 1991 (1986) version, EV=Engel-Vosko, and BP=Becke-Perdew.

| Reference | Potential | $a_0$ | $E_0$ | $B_0$ |
|---|---|---|---|---|
| Expt. | | 7.60[a] | 3.37[b] | 72.7[c] |
| Nonrel. LDA | | | | |
| Present | HL | 7.60 | 4.07 | 79.7 |
| Ref. 17 | HL | 7.60 | 3.88 | 80 |
| Ref. 18 | W | 7.58 | 3.65 | 71.5 |
| Ref. 3 | KSG | 7.65 | 3.20 | 96.8 |
| Ref. 19 | PZ | 7.43 | 4.14 | 87.6 |
| Relat. LDA | | | | |
| Ref. 20 | HL | 7.54 | 4.01 | 82.2 |
| Ref. 21 | HL | 7.54 | | 84 |
| Ref. 22 | PZ | 7.52 | 4.16 | 83.9 |
| Ref. 23 | PZ | 7.48 | 4.05 | 87 |
| GDA | | | | |
| Ref. 19 | PW91 | 8.03 | 3.22 | 61.1 |
| Ref. 24 | PW91 | 7.62 | 3.45 | 79.3 |
| Ref. 21 | PW91 | 7.65 | | 74 |
| Ref. 22 | PW91 | 7.74 | 3.74 | 72.6 |
| Ref. 23 | PW86 | 7.63 | 3.09 | 79 |
| Ref. 21 | EV | 7.91 | | 55 |
| Ref. 23 | BP | 7.65 | 3.23 | 77 |

[a]Static lattice value deduced from experiment in Ref. 18.
[b]Static lattice value deduced from experiment in Ref. 3.
[c]Reference 7.

lations, it seems safe to conclude that any high-precision, all-electron, full-potential, nonrelativistic LDA (beyond KSG) calculation for fcc Al should produce an equilibrium lattice constant of $7.60 \pm 0.02$ bohr, a binding energy of $4.0 \pm 0.2$ eV/atom, and a bulk modulus of $80 \pm 4$ GPa.

The relativistic LDA results in Table III also show a very high degree of consistency; especially if the one pseudopotential result (from Ref. 23) is dropped from consideration. Comparison of the first three sets of results suggests that any high-precision, all-electron, full-potential, relativistic LDA calculation for fcc Al should produce a lattice constant of $7.53 \pm 0.02$ bohr, a binding energy of $4.1 \pm 0.1$ eV/atom, and a bulk modulus of $83 \pm 3$ GPa. Although the relativistic and nonrelativistic calculations produce essentially the same binding energy and bulk modulus, the relativistic lattice constants are significantly smaller than both the nonrelativistic calculated values and the measured ones.

Perhaps the most intriguing result in Table III is the lack of any clear trend in the results obtained with the various GDA calculations. The most that can be said with any certainty is that the GDA binding energy is much closer to experiment than the LDA binding energy. The calculated lattice constants range from 7.63 bohr to 8.03 bohr, while the calculated bulk modulii range from 55 to 79.3 GPa. Since the lattice constants and bulk modulii calculated with a single GDA span a wide range of values, it seems likely that the scatter in the results reflects a high sensitivity to matters of computational art in the density-gradient calculations required by the GDA's. A likely source for this sensitivity would be the residual discontinuity in the calculated density-gradient and GDA potential at the boundary between the muffin-tin and interstitial regions that are utilized in many modern cellular-based techniques or the core-valence corrections required in the case of the pseudopotential technique. Neither of these approximations is used in GTOFF, though GDA's have not yet been implemented in it.

### B. Equation of state for fcc Al

The fact that electronic-structure calculations yield a $T=0$ K static-lattice isotherm, whereas available experiments generally measure pressure-volume curves at several hundred Kelvin, makes direct comparison of experiment and theory difficult. To allow a meaningful assessment of the parametrized EOS's given in Table II, a theoretical 300-K isotherm for fcc Al was generated by adding nuclear motion contributions to the static-lattice 0-K isotherm. The phonon contributions were obtained from a global EOS for Al stored in the well-known SESAME EOS library at Los Alamos National Laboratory.[25] The static-lattice 0-K isotherm given in Table II and the 300-K isotherm derived from it are both shown in Fig. 1, along with room-temperature DAC data[7] and a 300-K isotherm deduced from Hugoniot data.[26]

Detailed examination of both panels of Fig. 1 reveals two important features of the theoretical 300-K isotherm. First, the thermal expansion produced by adding the phonon contributions shifts the calculated volume at zero pressure into nearly perfect agreement with the measured (ambient temperature) volume for fcc Al, $V_{300}=112.0$ a.u.[26] Second, the calculated 300-K isotherm appears to be somewhat stiffer than both of the measured isotherms. That slight difference is rather unsurprising given the fact that the underlying theoretical bulk modulus is roughly 10% larger than the experimental value (see Table III). Because the difference between the theoretical 0- and 300-K isotherms is very small, the 0 K isotherm is actually in slightly better agreement with the room-temperature data.

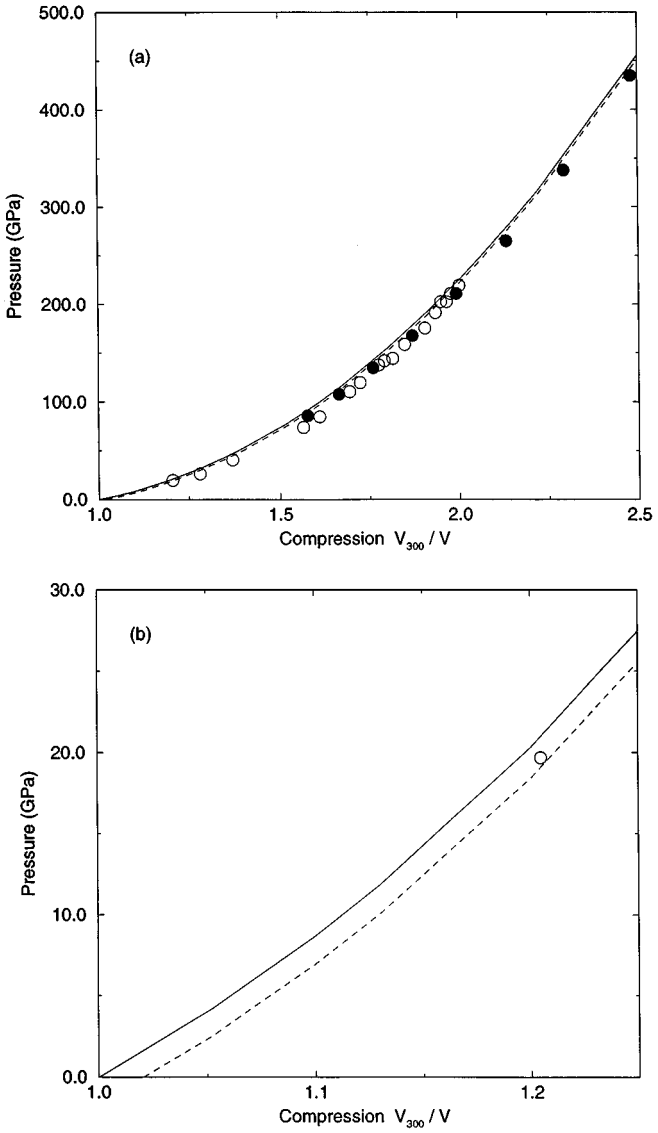


FIG. 1. The theoretical static-lattice 0-K isotherm calculated here (dashed line) and the 300-K isotherm derived from it (solid line), compared with room-temperature diamond-anvil-cell measurements (Ref. 7, open circles) and a 300-K isotherm deduced from shock data (Ref. 26, solid circles); (a) over the full range of the data and (b) for the low-pressure region. Compressions are given relative to the measured zero pressure volume at 300 K; $V_{300}=112.0$ a.u.

Relative to the shock data, the calculation overestimates the pressure from as little as 2.5% for the largest measured pressure (435 GPa) to as much as 6.4% at the smallest measured pressure (86 GPa). Thus, the theoretical 300-K isotherm lies well within the estimated error bars for the shock data, $\pm 10\%$,[26] and tracks those data smoothly with a deviation that decreases with increasing pressure. Although the theoretical 300-K isotherm is in excellent agreement with the DAC data for the lowest measured pressure and for the five

TABLE IV. LCGTO-FF predictions (this work) for the static lattice structural phase transition pressures ($P$; in GPa) and relative volumes ($V/V_{300}$; $V_{300}$=112.0 a.u.) are compared with previous calculations using the GPT (Ref. 1), LMTO-ASA (Ref. 1), AP (Ref. 2), and LCGTO (Ref. 3) methods. An experimental lower bound for the room-temperature fcc→hcp transition from Ref. 7 is given also.

| | Fcc→hcp | | Hcp→bcc | | Fcc→bcc | |
|---|---|---|---|---|---|---|
| | $P$ | $V/V_{300}$ | $P$ | $V/V_{300}$ | $P$ | $V/V_{300}$ |
| LCGTO-FF | 205±20 | 0.510 | 565±60 | 0.364 | 340±15 | 0.436 |
| GPT | 360 | | 560 | | | |
| LMTO-ASA | 120 | | 200 | | | |
| AP | 220 | 0.50 | 380 | 0.40 | 300 | 0.45 |
| LCGTO | | | | | 330 | 0.446 |
| Expt. | >219 | <0.50 | | | | |

highest measured pressures, Fig. 1 shows that the overall agreement is not as good as for the shock data. In particular, both the calculated EOS and the shock data lie above the intermediate pressure DAC points. Greene, Luo, and Ruoff[7] found the same behavior in fitting the $H11$ EOS form to their data: see the inset to their Fig. 2. As Greene, Luo, and Ruoff, also noted, the fitted $H11$ EOS is in excellent agreement with the shock data. Correspondingly, that $H11$ fit to the DAC data and our calculated isotherm differ by no more than 7% (relative to $H11$). The remaining differences between our isotherm and the raw data in Ref. 7 seem to be simply the consequence of a modest amount of scatter in the intermediate pressure DAC data. In light of these considerations, the calculated 300-K EOS seems to be in satisfactory agreement with both experiments.

### C. Crystallographic phase stability

Transition volumes and pressures for the fcc→hcp and fcc→bcc transitions were determined from crossings of enthalpy vs pressure curves obtained from the parametrized static-lattice EOS's in Table II. The fcc→hcp transition is predicted to occur at 205±20 GPa with $V/V_{300}$=0.510 ($V$ =the average volume during the transition), while the fcc→bcc transition occurs at 340±15 GPa with $V/V_{300}$=0.436. The error bars on these pressures assume a 0.5 mRy uncertainty in the structural energy difference including both EOS fitting and BZ integration errors.

Because the calculated hcp→bcc transition lay outside the range of volumes considered in the first fit, the EOS's for the three structures were refitted including one more cohesive energy, corresponding to an fcc lattice constant of 5.35 bohr (see Table I). The new EOS's yielded an hcp→bcc transition pressure of 565±60 GPa ($V/V_{300}$=0.364). The larger error margin for this transition pressure reflects an increased standard deviation for the EOS fits, and an overall uncertainty of 1.0 mRy in the relevant structural energy difference. The cohesive energies in Table I suggest that above the hcp→bcc transition, the bcc phase will remain the most stable of the three phases up to the highest compression considered here. A finite difference calculation of the pressure in the bcc phase at $a_{bcc}$=4.0515 bohr ($V/V_{300}$=0.297) yielded 1.022 TPa, which compares well with the 300 K pressure of 1.018 TPa at $V/V_{300}$=0.304 deduced from shock wave data.[26]

All of the current predictions for the crystallographic phase transitions in Al are summarized in Table IV and are compared with the results of previous calculations and experiment. It is quite reassuring that the only previous all-electron, full-potential prediction[3] for the fcc→bcc transition pressure lies within the current error bars, in spite of the coarser BZ mesh used in the earlier LCGTO calculations. More importantly, the present fcc→hcp transition pressure is in good agreement with the intermediate prediction of Lam and Cohen;[2] see the discussion above. This means that there is no obvious inconsistency between the ''best'' LDA prediction and the experimental lower bound for the fcc→hcp transition pressure. In addition, the LDA predicts a transition pressure that is within the reach of DAC experiments.

Since the upper limit for the static-lattice fcc→hcp transition pressure is barely above the lower bound determined in the DAC experiment,[7] a careful analysis of the prediction is warranted. First, consider the uncertainty due to the choice of LDA model. To test for sensitivity to that choice, $E_{fcc}-E_{bcc}$ was recalculated at $a_{fcc}$=7.60 bohr using the KSG model. This modification in the LDA produced a shift of only 0.05 mRy in the structural energy difference at $P$=0. This shift should decrease rapidly as the pressure is increased, since LDA models primarily differ in regions of low-electron densities. Thus, the sensitivity of the transition pressure to the choice of the LDA model should be negligible compared to other effects.

As already noted in the discussion of the EOS, an important distinction between the present calculation and the experiment is the neglect of phonon contributions, both zero point and thermal, in the underlying calculation. The global EOS for Al stored in the SESAME EOS library[25] has a total phonon energy of 9 mRy (10 mRy) for $T$=0 K (300 K) at $V/V_{300}$=0.50. Even if the phonon energies for the close-packed structures differed by as much as 15%, the uncertainty in the structural energy difference on the 0- and 300-K isotherms from neglect of nuclear motion near the transition volume would be no more than 1.5 mRy. The estimated combined uncertainty in the fcc→hcp structural energy difference near the transition therefore is 2.0, 0.5 mRy from computational imprecision and 1.5 mRy from neglecting the phonons.

If the calculated enthalpy vs pressure curve for the hcp structure were to be shifted upward by that 2.0 mRy relative to the fcc curve, the transition pressure would be about 282 GPa. That value should then provide a reasonable upper bound for the $T$=0 K fcc→hcp transition pressure. Assuming

that the entropies for the two close packed structures are nearly the same, and adding in the 4 GPa nuclear contribution to the pressure on the 300-K isotherm at $V/V_{300}=0.50$, produces a rather firm upper bound of 290 GPa for the room temperature fcc→hcp transition in Al. Since this theoretical upper bound is only 70 GPa above the experimental lower bound, it is likely that the recent DAC experiments came close to, but just short of, observing the fcc→hcp transition.

## IV. CONCLUSIONS

These calculations of the EOS and structural phase stability of Al up to 1 TPa suggest a number of important conclusions. First, the fitted EOS's for fcc, hcp, and bcc Al given in Table II should provide a very realistic representation of the properties of Al for pressures ranging up to 450 GPa. In particular, the current nonrelativistic LDA calculations produce an equilibrium lattice constant that is in near perfect agreement with experiment; i.e., without the usual LDA-induced lattice contraction. In this regard, nonrelativistic LDA calculations might provide a better tool for studying Al than either relativistic LDA or GDA calculations in applications requiring a very accurate determination of Al-Al bond lengths. The most serious defects in the parametrized LDA EOS's are a 10% overestimate of the ambient bulk modulus and a *possible* 7% overestimate of the pressures in the 50→200 GPa range, which then rapidly decreases with increasing pressure.

The present LCGTO-FF phase stability calculations have confirmed the earlier predictions for the pressure induced crystallographic phase sequence in Al, fcc→hcp→bcc, and have reduced the uncertainties in the predicted transition pressures substantially; 205±20 GPa and 565±60 GPa. When the prediction for the static-lattice fcc→hcp phase transition is combined with a rather generous estimate of the possible impact of phonons on the transition pressure, a fairly firm upper bound of 290 GPa can be placed on the *room-temperature* fcc→hcp transition pressure in Al. (The corresponding $T=0$ K value is 282 GPa.) Hopefully this prediction will provide incentive for additional efforts to achieve the fcc→hcp transition experimentally.

## ACKNOWLEDGMENTS

J.C.B. thanks Duane Wallace for helpful discussions. S.B.T. thanks Ray Greene for providing unpublished numerical data for Ref. 7 and Alex Khein for providing unpublished cohesive energy values for Ref. 22. J.C.B. was supported by the U.S. Department of Energy. S.B.T. was supported in part by the U.S. Army Office of Research.

[1] A. K. McMahan and J. A. Moriarty, Phys. Rev. B **27**, 3235 (1983); J. A. Moriarty and A. K. McMahan, Phys. Rev. Lett. **48**, 809 (1982).
[2] P. K. Lam and M. L. Cohen, Phys. Rev. B **27**, 5986 (1983).
[3] J. C. Boettger and S. B. Trickey, Phys. Rev. B **29**, 6434 (1984).
[4] The Lam and Cohen values used here and throughout are taken from their Fig. 3, since their text cites approximate values only.
[5] L. Hedin and B. I. Lundqvist, J. Phys. C **4**, 2064 (1971).
[6] W. Kohn and L. J. Sham, Phys. Rev. **140**, A1133 (1965); R. Gaspar, Acta Phys. Hung. **3**, 263 (1954).
[7] R. G. Greene, Huan Luo, and A. L. Ruoff, Phys. Rev. Lett. **73**, 2075 (1994).
[8] J. C. Boettger and S. B. Trickey, Phys. Rev. B **51**, 15 623 (1995).
[9] J. C. Boettger (unpublished).
[10] J. C. Boettger, Int. J. Quantum Chem. Symp. **27**, 147 (1993); also see, J. C. Boettger and S. B. Trickey, Phys. Rev. B **32**, 1356 (1985); and J. W. Mintmire, J. R. Sabin, and S. B. Trickey, *ibid*. **26**, 1743 (1982).
[11] U. Birkenheuer, J. C. Boettger, and N. Rösch, J. Chem. Phys. **100**, 6826 (1994); U. Birkenheuer, Ph.D. thesis, TU München, 1994.
[12] J. C. Boettger, U. Birkenheuer, N. Rösch, and S. B. Trickey, Int. J. Quantum Chem. Symp. **28**, 675 (1994).
[13] J. C. Boettger, U. Birkenheuer, S. Kruger, N. Rösch, and S. B. Trickey, Phys. Rev. B **52**, 2025 (1995).
[14] L. Kleinman, Phys. Rev. B **28**, 1139 (1983); O. Jepsen and O. K. Andersen, *ibid*. **29**, 5965 (1984).
[15] H. J. F. Jansen and A. J. Freeman, Phys. Rev. B **30**, 561 (1984).
[16] A. Banerjea and J. R. Smith, Phys. Rev. B **37**, 6632 (1988).
[17] V. L. Moruzzi, J. F. Janak, and A. R. Williams, *Calculated Electronic Properties of Metals* (Pergamon, New York, 1978).
[18] P. K. Lam and M. L. Cohen, Phys. Rev. B **24**, 4224 (1981).
[19] Y. M. Juan and E. Kaxiras, Phys. Rev. B **48**, 14 944 (1994).
[20] M. Sluiter, G. De Fontaine, X. Q. Guo, R. Podloucky, and A. J. Freeman, Phys. Rev. B **42**, 10 460 (1990).
[21] P. Dufek, P. Blaha, and K. Schwarz, Phys. Rev. B **50**, 7279 (1994).
[22] A. Khein, D. J. Singh, and C. J. Umrigar, Phys. Rev. B **51**, 4105 (1995).
[23] A. Garcia, C. Elsässer, J. Zhu, S. G. Louie, and M. L. Cohen, Phys. Rev. B **46**, 9829 (1992).
[24] Y. M. Juan, E. Kaxiras, and R. G. Gordon, Phys. Rev. B **51**, 9521 (1995).
[25] The phonon contributions used here were taken from SESAME EOS material number 3718. See, for example, SESAME: The Los Alamos National Laboratory Equation Of State Database, edited by S. P. Lyon and J. D. Johnson (Los Alamos National Laboratory Document LA-UR-92-3407, 1992).
[26] W. J. Nellis, J. A. Moriarty, A. C. Mitchell, M. Ross, R. G. Dandrea, N. W. Ashcroft, N. C. Holmes, and G. R. Gathers, Phys. Rev. Lett. **60**, 1414 (1988).